



Characteristics of secondary particles in dC-, CC-, and CTa-collisions at a momentum of 4.2 GeV/c per nucleon

M.U.Sultanov, U.T.Usarov, G.Yu.Nodirov, J.T.Parmanov I.M.Egamberdiyev

Senior teacher Samarkand State Architecture and Construction University
Professor of Samarkand State Architecture and Construction University
Teacher of Samarkand State Architecture and Construction University
Teacher of Samarkand State Architecture and Construction University

ABSTRACT: In this study, the rapidity spectra of secondary hadrons (protons and π^- mesons) were analyzed, focusing on the interpretation of the spectra of protons and π^- mesons. The rapidity spectra of negative pions in dC-, CC-, and CTa-collisions were approximated using a Gaussian function. Experimental data were compared with theoretical predictions made by the Quark-Gluon String Model (QGSM). The QGSM was found to satisfactorily describe both the width and the central positioning of y_0 rapidity distributions of negative pions in dC-, CC-, and CTa-collisions at 4.2 GeV/c per nucleon. It was observed that the rapidity distributions of protons involved in these collisions underwent significant changes as the centrality of the collisions increased. The QGSM model was able to adequately predict the variation in the shape of the rapidity spectra of the involved protons as the centrality increased in the mentioned collisions [1, 2].

KEY WORDS: Hadron, Spectrum, Participant Protons, Approximation, Rapidity, Momentum

I. INTRODUCTION

A primary area of focus is the complex phenomenon of multiple particle production. This aspect is complex and requires thorough analysis due to the ongoing developments in theories related to hadron quark structure and the dynamics of strong interactions. Recently, there has been an increase in the consideration of nucleus-nucleus collisions as a series of individual hadron-nucleus collisions. This model has been effective in explaining the characteristics of various secondary particles across a broad energy spectrum. However, experimental data often contradict this straightforward interaction model, leading to questions about the specific conditions under which new properties of this process become apparent. For a deeper understanding, it is essential to gather detailed data on hadron-nucleus and nucleus-nucleus collisions, especially data that allows precise control over the impact parameter. Such data will pave the way for a comprehensive and nuanced understanding of these complex collision events [3, 4]. The data sets for this experiment were obtained using a two-meter propane chamber. This chamber was irradiated by beams of deuterium (^2H) and carbon (^{12}C) nuclei, each with a momentum of 4.2 GeV/c per nucleon. These data sets contain detailed information about the types of secondary particles generated and their kinematic characteristics. The methodological aspects of the experiment, which include the selection of interactions involving the carbon nucleus from all recorded events in the propane, the identification of particles, and the application of geometric corrections for particles lost due to emission at large angles to the plane of photography, are discussed in references [5, 6].

II. RESULTS AND DISCUSSIONS

In the interactions under consideration, several types of secondary particles were identified. These included π^+ and π^- mesons, evaporative protons (protons with a momentum less than 0.3 GeV/c), stripping fragments from the incident carbon nucleus (having momenta greater than 3 GeV/c and an emission angle $\theta < 3^\circ$), and participating protons (with a momentum greater than 0.3 GeV/c, excluding stripping particles). The study also focused on the behavior of protons with a momentum in the range of $0.3 \leq p < 0.75$ GeV/c, identified as participating protons from the target, and protons with a momentum of $p > 0.75$ GeV/c, identified as participating protons from the projectile nucleus. In table 1 is

shown number of events in nuclear-nuclear collisions for analyses. This process effectively excluded all slow particles that would be absorbed in a 2-mm layer of propane and in tantalum foil.

Table 1. The statistical materials of investigation

Intractions	dC	CC	CTa
Experiment	7070	20527	2420
QGSM	30000	30000	6000

The rapidity of π^- mesons

Table 2 shows the average multiplicities of negative pions and participating protons, alongside the average rapidity and transverse momentum values for π^- -mesons in dC-, CC-, and CTa-collisions at 4.2 GeV/c per nucleon. These averages are derived from both experimental observations and calculations based on the Quark-Gluon String Model (QGSM). The average rapidity values are computed within the center-of-mass system (c.m.s.) of nucleon-nucleon collisions.

Table 2. Experimental and QGSM model results for negative pion multiplicities

Type of interaction	$\langle n_{\pi^-} \rangle$	$\langle n_{part.pr} \rangle$	$\langle y_{c.m}(\pi^-) \rangle$	$\langle p_t(\pi^-) \rangle$ (GeV/c)
dC, experiment.	0.64±0.01	1.97±0.02	-0.12±0.01	0.250±0.003
QGSM	0.62±0.01	1.88±0.01	-0.16±0.01	0.220±0.002
CC, experiment.	1.47±0.01	4.28±0.02	-0.015±0.005	0.243±0.001
QGSM	1.56±0.01	4.01±0.02	0.008±0.005	0.216±0.001
CTa, experiment.	3.53±0.10	13.7±0.2	-0.35±0.01	0.209±0.002
QGSM	5.07±0.09	14.1±0.2	-0.31±0.01	0.183±0.001

The comparison between the experimentally obtained and QGSM-calculated rapidity distributions of negative pions in dC-, CC-, and CTa-collisions at a momentum of 4.2 GeV/c per nucleon is depicted in tab.2, The rapidity of the center of mass for nucleon-nucleon collisions $y_{c.m.s.} \approx 1.1$, corresponding to the same momentum value of the incident particle. Notably, the rapidity distribution of negative pions in CC-collisions symmetrically spans around the central rapidity value $y_{c.m.s.} = 0$. This symmetry is expected in systems where the projectile and target nuclei are identical. The peak of the rapidity distribution, and consequently the multiplicity of π^- -mesons, escalates with the increasing mass of the projectile and target nuclei. The rapidity distribution of π^- -mesons shifts towards lower rapidities or more towards the target fragmentation region, especially as the target nucleus mass increases from CC to CTa-collisions. This shift is attributable to the growing effective number of participating target nucleons, thereby increasing the number of π^- -mesons forming in the target fragmentation region. The QGSM is shown to satisfactorily replicate the experimental rapidity distributions of π^- -mesons in dC, CC, and CTa collisions. The experimental rapidity spectra of negative pions in the analyzed collisions can be approximated by a Gaussian function as follows [9,10]:

$$F(y) = \frac{A_0}{\sigma} \exp\left(\frac{-(y - y_0)^2}{2\sigma^2}\right), \tag{1}$$

where σ – is the standard deviation, referred to as the distribution width in this work, y_0 – is the center of the Gaussian distribution, and A_0 is the approximation constant. The parameters obtained from the approximation of the rapidity spectra of negative pions in dC-, CC-, and CTa-collisions at 4.2 GeV/c per nucleon by the Gaussian function shown in equation (1) are presented in Table 3. As seen from Table 3, the widths of the rapidity distributions of π^- -mesons almost coincide in dC and CC-collisions, while they are somewhat smaller in CTa-collisions, both in the experiment and

in the QGSM. The width of the experimental rapidity spectra of negative pions ($\sigma^{C+C} = 0,793 \pm 0,003$ and $\sigma^{C+Ta} = 0,75 \pm 0,01$), obtained from this analysis, turned out to be slightly smaller than the corresponding widths ($\sigma^{C+C} \approx 0,82$ and $\sigma^{C+Ta} \approx 0,79$), estimated in works [3,4] for CC- and CTa-collisions at 4.2 GeV/c, based on full experimental statistics, which was half of the corresponding statistical material used in the current work. From Table 3, it is evident that the positioning of the centers y_0 , obtained from the approximation of the rapidity spectra of π^- -mesons by the Gaussian function, coincides within the margin of error with the corresponding average rapidity values of negative pions in the analyzed collisions, as shown in Table 3.

Table 3. Gaussian fit parameters for negative pion rapidity spectra in dC-, CC- and CTa-collisions at 4.2 GeV/c per nucleon with corresponding degrees of freedom and goodness-of-fit measures

Type of interaction	A_0	σ	y_0	$\chi^2/n.d.f.$	R^2 factor
dC, experiment.	0.250±0.004	0.77±0.01	-0.11±0.01	2.86	0.981
QGSM	0.248±0.003	0.79±0.01	-0.16±0.01	5.11	0.982
CC, experiment.	0.582±0.004	0.788±0.003	-0.014±0.005	8.91	0.990
QGSM	0.612±0.004	0.782±0.003	0.008±0.005	13.11	0.981
CTa, experiment.	1.38±0.02	0.76±0.01	-0.32±0.01	7.66	0.970
QGSM	1.76±0.02	0.72±0.01	-0.30±0.01	23.43	0.877

As indicated in Table 4, the QGSM satisfactorily describes both the width and the positioning of y_0 in the rapidity distributions of negative pions in dC-, CC-, and CTa-collisions at 4.2 GeV/c per nucleon.

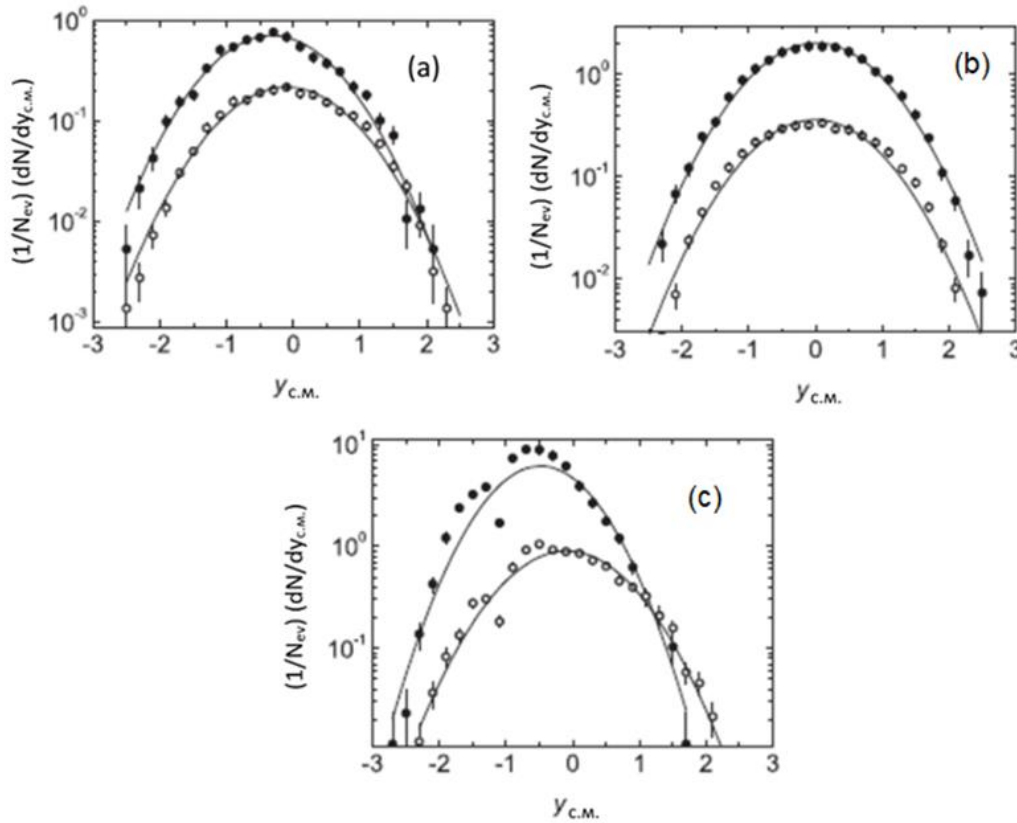
Conducting a quantitative analysis to understand how the rapidity spectra of negative pions change as collision centrality increases, corresponding to a decrease in the collision impact parameter, is of significant interest. For assessing collision centrality, we utilize the count of participating protons, referred to as $n_{pr.part}$. This approach aligns with methodologies outlined in reference [3,4], where peripheral collision events are defined as those with $n_p \leq \langle n_{pr.part} \rangle$, and central collision events are those with $n_p \leq 2 < n_{pr.part} \rangle$, where $\langle n_{pr.part} \rangle$ is the average multiplicity of participating protons. Reference [5] demonstrated that in central CTa-collisions at 4.2A GeV/c, identified using these criteria, the projectile was completely stopped. This outcome was evident as the average number of interacting projectile nucleons, denoted as $\langle \nu^p \rangle$, closely matched the total nucleon count in the carbon projectile nucleus. Table 4 in this study presents the proportion of central and peripheral dC-, CC-, and CTa-collisions relative to the total inelastic cross-section, based on both experimental data and QGSM findings. As Table 3 illustrates, the proportion of experimental and QGSM-modeled central and peripheral events in dC-, CC-, and CTa-collisions generally align within two standard errors. The notable exception is the QGSM's slight overestimation of peripheral dC-collisions. According to the data in Table 4, central interactions account for about 10% of dC- and CC-collisions, and approximately 15% of CTa-collisions. Conversely, peripheral collisions comprise an estimated 60% of the collisions under analysis.

Table 4. Proportion of central and peripheral collisions in dC-, CC-, and CTa- at 4.2 GeV/c per nucleon relative to the total inelastic cross-section

Type of interaction	Central collisions (%)		Peripheral collisions (%)	
	Experiment	QGSM	Experiment	QGSM
dC	10±1	12±1	53±1	73±1
CC	11±1	8±1	58±1	62±1
CTa	16±1	15±1	60±2	56±1

Figures 1 and 2 present a comparison of the rapidity distributions of negative pions for central and peripheral dC-, CC-, and CTa-collisions in both the experiment and QGSM, respectively. All spectra in Figures 2 and 3 are approximated by the Gaussian function presented in equation (1). The corresponding parameters extracted from the experimental spectra and

QGSM spectra for central and peripheral collisions are listed in Table 4. In general, as seen from Figures 2 and 3 and Table



5, all spectra are satisfactorily approximated by the Gaussian function. As indicated in Table 4, the widths of the experimental rapidity spectra of negative pions decrease by $(8 \pm 2)\%$, $(5 \pm 1)\%$, and $(15 \pm 2)\%$ when transitioning from peripheral to central dC-, CC-, and CTa-collisions, respectively.

A similar decrease in the calculated widths of the rapidity spectra of negative pions was observed in work [14] when transitioning from peripheral to central CC- and CTa-collisions at 4.2A GeV/c. The estimated widths for peripheral and central CC- and CTa-collisions, obtained in work [8], were found to be slightly larger compared to the corresponding widths of the experimental rapidity spectra shown in Table 4. As seen in Figures 2a, 2c, and Table 4, the centers y_0 of the

Fig. 1. Experimental rapidity distributions of negative pions in central (●) and peripheral (○) collisions of dC(a), CC(b), and CTa(c) at 4.2A GeV/c. The corresponding Gaussian function approximations are indicated with solid lines. All spectra are obtained in the center-of-mass system from nucleon-nucleon collisions at 4.2 GeV/c.

This absence of shift is probably due to the symmetry in the carbon-carbon colliding system. In this system, the effective number of participating nucleons in both the target and projectile remains nearly constant, regardless of whether the collisions are central or peripheral. Consequently, the rapidity distribution of negative pions in CC-collisions maintains its symmetry around $y_{c.m.s.} = 0$, even as the centrality of collisions increases. Furthermore, as indicated in Table 5, the peaks and centers y_0 of the rapidity spectra of π^- -mesons in peripheral dC- and CTa-collisions are observed to be close to $y_{c.m.s.} = 0$. This proximity might be due to the similar effective volumes of the interacting regions in the target and projectile nuclei in peripheral collisions, leading to comparable numbers of interacting nucleons in both nuclei.

III. CONCLUSION

The study's comparative analysis of the rapidity characteristics of negative pions in central dC-, CC-, and CTa-collisions yields several insightful conclusions. It is observed that the centers of the rapidity distributions of π^- -mesons, which are



approximated by a Gaussian function, align closely with the corresponding average rapidity values of negative pions from the collisions examined. This alignment within the error margin suggests that the rapidity spectra of negative pions are symmetric around their central values. Moreover, the distribution widths for π^- -mesons are found to be nearly identical in both dC and CC collisions, with slightly smaller widths in CTa collisions. These results are consistent with both the experimental data and the predictions from the Quark-Gluon String Model (QGSM). Interestingly, a decrease in the widths of the experimental rapidity spectra of negative pions is noted when moving from peripheral to central collisions across all three types studied. The analysis further reveals that the centers of the experimental rapidity distributions of π^- -mesons shift towards the target fragmentation region, specifically by -0.32 ± 0.04 units in central dC-collisions and by -0.44 ± 0.02 units in central CTa-collisions. These shifts are described to the increased rescattering effects in the heavier target nuclei relative to the projectile nuclei. As the centrality of the collisions increases, so does the number of participating target nucleons, which in turn augments the number of pions formed in the target fragmentation region. This trend underscores the influence of collision centrality on the dynamic processes within these interactions. Furthermore, the QGSM model proves to be highly effective in describing the experimental data of negative pions across dC, CC, and CTa collisions at 4.2 GeV/c per nucleon. The model's success in capturing the essential features of the spectra underscores its utility and precision in simulating the complexities inherent in such high-energy particle interactions. Overall, these findings enhance our understanding of hadron-nucleus and nucleus-nucleus collisions, contributing valuable insights into the behavior of π^- -mesons within these environments.

REFERENCES

1. Togayev I., Tursunova A., Eshmirzayev M. Monitoring of overhead power lines //international conference: problems and scientific solutions. 2022. -T. 1. - №. 2. - c. 267-271.
2. Akram T., Islomjon T., Shahrizoda R. Energy Problems in uzbekistan. Their solutions and remedial measures //Yosh Tadqiqotchi Jurnal. - 2022. - T. 1. - №. 2. - C. 273-277.
3. Ibodulaev, M., Tovboyev, A.N. Research of Ferro-Resonance Oscillations at the Frequency of Subharmonics in Three-Phase Non-Linear Electric Circuits and Systems//E3S Web of Conferences, 2020, 216, 01113 https://www.e3sconferences.org/articles/e3sconf/pdf/2020/76/e3sconf_rses2020_0113.pdf
4. Tog'ayev I.B., Isoqulov D.SH., Turniyozov Z.A. Monitoring of air power lines with an assessment of their condition // Central Asian Research Journal For Interdisciplinary Studies (CARJIS) ISSN (online): 2181-2454 Volume 2 | Issue 5 | May, 2022
5. Islomjon Bekpo'lat o'gli Togayev, and Tovbaev Akram Nurmonovich. "statistical analysis of power waste on 6-10 kv air power transmission lines." international journal on orange technologies 2.10: 92-94.
6. I Togayev, A Norqulov, S Shirinov. modern technologies for improving the quality of electricity. Results of national scientific research international journal 2 (2), 177-181
7. T Akram, T Islom, U Islombek. analysis of the impact of the installation of reactive power sources on the quality of electricity. Web of semantic: universal journal on innovative education 2 (2), 198-201
8. Bradnova V. et al. Nuclear Physics. A. 734, E92 (2004).
9. A.I.Bondarenco et al. The Ensemble of interactions on carbon and hydrogen nuclei obtained using the 2 m propane bubble chamber exposed to the beams of protons and H-2, He-4, C-12 relativistic nuclei at the Dubna Synchrotron (Dubna, 1998), JINR Preprint No. P1-98-292.
10. Simić Lj, Backović, Agakishiyev H.N., Kladnitskaya E.N., Cheplakov A.P. Influence of the collision centrality upon negative particle production in dC, α C, CC and CTa interactions at 4.2 GeV/c per nucleon. Z.Phys, 2016.
11. Akhtar Iqbal, Khusniddin Olimov, Mushtaq Ahmad, Ali Zaman, Obaidullah Janand B. S.
12. Yuldashev. Centrality and rapidity dependences of negative pions in He-C collisions at 4.2 A. GeV/c. Modern Physics Letters A. Vol. 34 (2019).
13. Kh.K.Olimov, K.Olimov, Sh.D.Tojimatov, F.K.Olimov, E.Kh.Bozorov, S.L.Lutpullayev, Sh.Z.Kanakova, M.Aliyev, M.Fazilov, B.S.Yuldashev. Centrality dependences of negative pions in $\pi^- + ^{12}\text{C}$ interactions at 40 GeV/c. Ukr. J. Phys. 2019. Vol. 64, No.2, p.93- 99
14. Kh.K.Olimov et al. International Journal Modern Physics. E23, 1450084 (2014).
15. R.Hagedorn and J.Raft, Nuovo Cimento, Suppl. 6, 169 (1968).
16. R.Hagedorn and J.Rafelski. Physics Letters. B97, 136 (1980).
17. Backovich et al. Phys.Rev. C 46, 1501 (1992)
18. Kh.K.Olimov et al. Physical Review C88, 064903 (2013)